

Construction of exact refinements for the two-dimensional HB/THB-spline de Rham complex

Diogo C. Cabanas^{a,*}, Kendrick M. Shepherd^b, Deepesh Toshniwal^a, Rafael Vázquez^c

^a *Delft Institute of Applied Mathematics, Delft University of Technology, The Netherlands*

^b *Civil & Construction Engineering, Brigham Young University, Provo UT 84602, USA*

^c *Department of Applied Mathematics, University of Santiago de Compostela, and Galician Centre for Mathematical Research and Technology (CITMAga), Santiago de Compostela, Spain*

Abstract

Studying the de Rham complex is a natural choice when working with problems in electromagnetics and fluid mechanics. By discretizing the complex correctly, it is possible to attain stable numerical methods to tackle these problems. An important consideration when constructing the discrete complex is that it must preserve the cohomology structure of the original one. This property is not guaranteed when the discrete function spaces chosen are hierarchical B-splines. Research shows that a poor choice of refinement domains may give rise to spurious harmonic forms that ruin the accuracy of solutions, even for the simplest partial differential equations. Another crucial aspect to consider in the hierarchical setting is the notion of admissibility, as it is possible to obtain optimal convergence rates of numerical solutions by limiting the multi-level interaction of basis functions. We will focus on the two-dimensional de Rham complex over the unit square $\Omega \subseteq \mathbb{R}^2$. In this scenario, the discrete de Rham complex should be exact, and we provide both the theoretical and the algorithm-implementation framework to ensure this is the case. Moreover, we show that, under a common restriction, the admissibility class of the first space of the discrete complex persists throughout the remaining spaces. Finally, we include numerical results that motivate the importance of the previous concerns for the vector Laplace and Maxwell eigenvalue problems.

1. Introduction

Over the last few years, there have been several developments in numerical methods designed to approximate the solution of partial differential equations (PDEs). Finite element exterior calculus (FEEC) [2, 3] is one of these developments; the theory has gained a lot of traction, since its earlier publications [4] due to its ability to describe how stable numerical methods can be achieved for a broad class of PDEs. Key elements used to ensure the stability of discrete methods are the topological and differential-geometric structure of PDEs, which are captured in FEEC through complexes and, more specifically, their cohomology classes. By choosing an appropriate finite element space, it is possible not only to approximate the continuous solution, but also to guarantee the method is stable — provided that the continuous and discrete complexes are cohomologically-equivalent.

Another important breakthrough in the field of numerical analysis was the introduction of spline functions [5, 29] as a compelling alternative to the more classical finite element method [24, 15, 7]. The former approach was given the name of isogeometric analysis (IGA), and it is explained in great detail in the seminal paper by T.J.R. Hughes, J. Cottrell and Y. Bazilevs [25]. The motivation behind this method was to create a better synergy between numerical-analysis and industrial-design teams — which have been using splines in

*Corresponding Author

Email addresses: d.costacabanas@tudelft.nl (Diogo C. Cabanas), kendrick_shepherd@byu.edu (Kendrick M. Shepherd), d.toshniwal@tudelft.nl (Deepesh Toshniwal), rafael.vazquez@usc.es (Rafael Vázquez)

CAD-based modelling for a long time [21]. One of the benefits of the higher smoothness allowed in splines is that they provide better approximation properties per degree of freedom (DoF) than standard C^0 or C^{-1} finite element spaces [19, 8, 27, 28]. Another upside in IGA is the flexibility in defining new spline spaces from basic splines, such as the B-spline; several of these have been explored in the literature: non-uniform rational B-splines (NURBS) [26], locally refined splines, such as T-splines [31, 30], hierarchical B-splines (HB-splines) [12, 17] and truncated hierarchical B-splines (THB-splines) [22], and the more recent polar splines [33].

For the sake of reasonable computation times, it is generally advisable to restrict regions with a high density of DoFs to relevant local features of the solution being computed. Locally-refined splines are naturally well-suited for problems where these localized features control the overall rate of converge of numerical solutions; one of the more common options being HB- and THB-splines. Both of these spline types can be used to describe the same discrete function space — where the advantages of one over the other depend on the application. In both cases, however, a local refinement without careful consideration can lead to error-convergence rates worse than the optimal ones predicted in the IGA framework. The most straightforward way to regain optimal convergence is to limit the interaction of basis functions from different refinement levels, using what is called admissibility [6].

When working with a hierarchical B-spline complex in $\mathbb{R}^n, n \geq 1$, it is not true in general that this complex will generate an exact subcomplex of the continuous one for an arbitrary refinement [20, 32]. This is due to the fact that a poor choice of refinement pattern can remove basis functions from a coarser level and add basis functions from a finer level such that they describe function spaces with distinct topological properties; leading to the introduction of spurious harmonic forms, which can easily ruin the accuracy and stability of the numerical method being used.

In this paper, we focus on providing an overview of the inexact refinements described above, as well as a way to add DoFs to the hierarchical B-spline de Rham complex that turns them into exact refinements. Many of the proofs that follow either work for a general hyper-cube, or can easily be adapted to do so, but we will mostly restrict ourselves to the two-dimensional case due to the significant simplifications of the computational implementation. The main contributions of this paper are as follows: we show that admissibility is preserved in the whole complex if it is preserved for the space of zero-forms in Lemmas 4.2 and 4.3; and we describe Algorithm 3, which provides the extra DoFs to a hierarchical basis that ensure an exact discrete subcomplex.

The structure of the paper is as follows: in Section 2 we give a basic overview of the de Rham complex and its discretization. Next, in Section 3 we describe the construction of hierarchical B-splines and the corresponding hierarchical B-spline de Rham complex. In Sections 4 and 5, we present the main theoretical results for admissibility and exactness, respectively. These are followed by Section 6 with their accompanying algorithms. We test our approach numerically in Section 7, where we showcase various examples: vector Laplace problem and Maxwell’s eigenvalue problem, both for illustrative, contrived cases and as an adaptive scheme. Finally, in Section 8 we give some concluding remarks.

2. Preliminaries

We start by introducing an overview of the basic objects and concepts used in FEEC. We specialize this overview for the two-dimensional case, which is our primary focus. Moreover, we simplify the exposition by avoiding the use of differential forms and instead use vector calculus proxies. For a more general discussion, the reader is invited to consult [1].

2.1. The Hilbert de Rham complex

Let $\Omega \subset \mathbb{R}^2$ be a bounded domain with a piecewise-smooth Lipschitz boundary. The following sequence, \mathfrak{R} , of Hilbert spaces and connecting differential operators is called the Hilbert de Rham complex,

$$\mathfrak{R} : H^1(\Omega) \xrightarrow{\text{grad}} \mathbf{H}(\text{curl}; \Omega) \xrightarrow{\text{curl}} L^2(\Omega) ,$$

where \mathbf{grad} is the gradient operator defined in coordinates by $\mathbf{grad} u = (\partial_x u, \partial_y u)$, curl is the scalar curl operator in two dimensions and is defined in coordinates as $\text{curl} \mathbf{v} := \partial_x v_2 - \partial_y v_1$, $L^2(\Omega)$ is the space of square-integrable functions on Ω , and

$$\begin{aligned} H^1(\Omega) &:= \{u \in L^2(\Omega) : \mathbf{grad} u \in [L^2(\Omega)]^2\} , \\ \mathbf{H}(\text{curl}; \Omega) &:= \{\mathbf{v} \in [L^2(\Omega)]^2 : \text{curl} \mathbf{v} \in L^2(\Omega)\} . \end{aligned}$$

We will refer to these spaces as $\mathbb{X}^0 = H^1(\Omega)$, $\mathbb{X}^1 = \mathbf{H}(\text{curl}; \Omega)$ and $\mathbb{X}^2 = L^2(\Omega)$.

The sequence \mathfrak{A} is called a complex because of two properties. First, each differential operator maps from one space into the next space,

$$\text{Im}(\mathbf{grad}) \subset \mathbf{H}(\text{curl}; \Omega) , \quad \text{Im}(\text{curl}) \subset L^2(\Omega) .$$

Second, the composition of the two operators is identically zero, or in other words, $\text{curl}(\mathbf{grad} f) = 0$ for any $f \in H^1(\Omega)$. Given these two properties, we can define the following (quotient) spaces called the cohomology spaces of \mathfrak{A} ,

$$H^0(\mathfrak{A}) := \text{Ker}(\mathbf{grad}) , \quad H^1(\mathfrak{A}) := \text{Ker}(\text{curl})/\text{Im}(\mathbf{grad}) , \quad H^2(\mathfrak{A}) := L^2(\Omega)/\text{Im}(\text{curl}) .$$

The elements of $H^k(\mathfrak{A})$ are called harmonic scalar/vector fields. These cohomology spaces are important because, first, they capture the topological properties of the domain Ω and, second, the solutions to scalar and vector Laplacians are well-defined up to harmonic fields. The following two paragraphs elaborate on this structure that underlies the Hilbert de Rham complex.

It turns out that there is a one-to-one correspondence between the cohomology spaces and the so-called Betti numbers of Ω : the vector space dimension of $H^j(\mathfrak{A})$ is equal to the number of j -dimensional holes in Ω . That is, $\dim H^0(\mathfrak{A})$ is the number of connected components of Ω , $\dim H^1(\mathfrak{A})$ is the number of holes in Ω , and $\dim H^2(\mathfrak{A}) = 0$ in our planar setting (since there are no two-dimensional holes in Ω). In particular, we will focus only on simply-connected domains Ω , which implies that $H^0(\mathfrak{A}) \cong \mathbb{R}$ and $H^1(\mathfrak{A}) = \emptyset = H^2(\mathfrak{A})$ in our setting.

The second reason why cohomology spaces are important is that harmonic fields in $H^1(\mathfrak{A})$ are the solutions to the homogeneous vector Laplace problem, $\Delta \mathbf{v} = 0$, and the harmonic fields in $H^0(\mathfrak{A})$ are the solutions to the homogeneous scalar Laplace problem, $\Delta u = 0$, with homogeneous natural boundary conditions. Given the assumption of simply-connectedness for Ω , this means that the homogeneous vector Laplace problem admits only the trivial solution, and only constant functions satisfy the homogeneous scalar Laplace problem.

2.2. Structure-preserving discretizations

The core principle of FEEC is to preserve the structural connections mentioned above in the discrete setting. This can be achieved by choosing appropriate finite element spaces for approximating scalar and vector fields. Failure to preserve the cohomological structure in the discrete setting can cause, in particular, spurious harmonic fields to appear in the discrete setting, which can lead to highly inaccurate solutions to scalar and vector Laplace problems. Examples can be found in Section 7 of this paper, and also in [1], for instance.

The FEEC recipe to preserve the cohomological structure is ensuring that the cohomology spaces of the discrete and continuous complexes can be isomorphically identified with maps that are bounded and commute with the operators defined above. By doing so, we can also ensure that we do not introduce any spurious harmonic scalar/vector fields, as these are intimately related with the cohomology spaces. In short, we want to construct a discrete version, \mathfrak{A}_h , of the de Rham complex \mathfrak{A} , namely,

$$\mathfrak{A}_h : \mathbb{X}_h^0(\Omega) \xrightarrow{\mathbf{grad}} \mathbb{X}_h^1(\Omega) \xrightarrow{\text{curl}} \mathbb{X}_h^2(\Omega) ,$$

for some appropriate choice of finite element spaces $\mathbb{X}_h^j(\Omega)$, $j \in \{0, 1, 2\}$, and where h is a parameter inversely proportional to the number of DoFs.

The relevant properties of these finite element spaces have been highlighted in [3, 1], and we showcase them here briefly for ease of readability. For a more comprehensive overview of the properties and corresponding results, we refer the reader to the works just mentioned. First, we require that the finite element spaces considered have enough similarity with the continuous ones to be able to approximate them arbitrarily well. To be concrete, we necessitate that

$$\lim_{h \rightarrow 0} \inf_{u_h \in \mathbb{X}_h^j} \|u_h - u\| = 0, \quad u \in \mathbb{X}^j, j \in \{0, 1, 2\}.$$

The second requisite is that the chosen discrete spaces, together with the operators of the complex \mathfrak{R} , also form a complex, or, in other words,

$$\mathbf{grad} \mathbb{X}_h^0 \subseteq \mathbb{X}_h^1, \quad \mathbf{curl} \mathbb{X}_h^1 \subseteq \mathbb{X}_h^2,$$

and the composition of the two operators is zero, as in the continuous case. The final property we mention here is crucial for the correct behaviour of a discrete solution, and is the one that establishes a connection between the cohomology spaces of the two complexes. That is, it should be possible to define a set of bounded projection maps from \mathfrak{R} to \mathfrak{R}_h , in such a way that a commuting diagram is formed. By guaranteeing the three properties listed above, one can ensure an accurate and stable solution of the mixed formulation of Laplace problems.

It is precisely this choice of appropriate finite element spaces that will be tackled in the rest of the paper, more specifically, when the finite element spaces are hierarchical B-spline spaces. Whether bounded commuting projectors exist for hierarchical B-spline complexes is still an open issue and outside the scope of the present work. We limit ourselves to characterizing and fixing the kind of refinements that introduce spurious harmonic forms, and therefore invalidate the existence of such projectors altogether.

3. Spline spaces

In this section, all required notation and definitions will be introduced for the univariate B-splines, and later extend into tensor product B-splines and, finally, the hierarchical B-spline de Rham complex. We will simplify the notation used in [20] and [32] to the two-dimensional case.

3.1. Univariate B-splines

In order to define univariate B-splines of polynomial degree $p \geq 1$, we need to define a knot vector. Namely, for $m \geq 1$, a knot vector $\Xi = (\xi_1, \dots, \xi_{m+p+1})$ is a sequence of non-decreasing real numbers, or knots, satisfying

$$\xi_1 = \dots = \xi_p < \xi_{p+1} \leq \dots \leq \xi_{m+1} < \xi_{m+2} = \dots = \xi_{m+p+1}.$$

We note that the first and last knots are repeated p times, which differs from the usual choice of $p+1$ repetitions, and enforces homogeneous boundary conditions for splines of degree p ; we also assume that no knot is repeated more than p times. To simplify the notation, we will consider that $\xi_1 = 0$ and $\xi_{m+p+1} = 1$ from now on.

The knot vector Ξ induces a partition of the interval $[0, 1]$, which we will denote by Z and call the breakpoints of Ξ . In other words, $Z = \{\zeta_1, \dots, \zeta_{z+1}\}$ is the largest subset of Ξ such that

$$\zeta_i < \zeta_{i+1}, \quad i \in \{1, \dots, z\}.$$

Also, it will be useful to define the intervals given by Z , namely

$$\mathcal{I} := \{(\zeta_i, \zeta_{i+1}) : i \in \{1, \dots, z\}\}. \tag{1}$$

Using the knot vector Ξ we can define two spaces that will be used to establish discrete complexes. Let $\mathbb{B}^0(\Xi)$ be the space of piecewise-polynomial functions of degree p and regularity C^{p-r} at knots with multiplicity r that vanish at $\xi \in \{0, 1\}$. Similarly, we set $\mathbb{B}^1(\Xi)$ as the space of piecewise-polynomial

functions of degree $p - 1$ with C^{p-r-1} regularity at knots with multiplicity r — no conditions imposed at the boundaries.

It is easy to see that, with the chosen boundary conditions, the dimension of the space $\mathbb{B}^j(\Xi)$ is $m + j$, $j \in \{0, 1\}$, and we can define a set of $m + j$ basis functions that span it. As mentioned in the introduction, we will choose to work with the B-splines B_i^j , $i \in \{1, \dots, m + j\}$, as the basis for $\mathbb{B}^j(\Xi)$, and denoting the set as $\mathcal{B}^j(\Xi)$. We refer the reader to [26, 29] for more details on the construction of B-splines. Nonetheless, we highlight a fact about the support of B-splines that will be used extensively throughout the paper:

$$\text{supp}(B_i^j) = (\xi_i, \xi_{i+p+1-j}), \quad j \in \{1, 2\}.$$

3.2. Tensor Product B-splines

Now that we have fully characterized univariate B-spline spaces, we can use them to construct a two-dimensional tensor-product B-spline space. Note that we will restrict the definitions and notation to these conditions, but the construction is altogether identical for higher-dimensional spaces.

Moreover, keeping in line with our desire to work with hierarchical spline spaces, we will also introduce the relevant notation for the levels of a hierarchy. We will use L to refer to the highest non-trivial refinement level and $0 \leq \ell \leq L$ for a general level.

Let $\mathcal{B}_\ell^{j_1}(\Xi_{\ell,1})$ and $\mathcal{B}_\ell^{j_2}(\Xi_{\ell,2})$ be two univariate spline spaces under the assumptions of Section 3.1. We denote their associated polynomial degrees and dimensions as $p_{(\ell,k)}$ and $m_{(\ell,k)} + j_k$, respectively, where $j_k \in \{0, 1\}$ and $k \in \{1, 2\}$. We can then define the tensor product space

$$\mathbb{B}_\ell^{\mathbf{j}} := \mathbb{B}^{j_1}(\Xi_{\ell,1}) \otimes \mathbb{B}^{j_2}(\Xi_{\ell,2}).$$

A basis for this space is given by

$$\mathcal{B}_\ell^{\mathbf{j}} := \left\{ B_{\mathbf{i},\ell}^{\mathbf{j}}(\xi_1, \xi_2) := B_{i_1}^{j_1}(\xi_1) B_{i_2}^{j_2}(\xi_2) : B_{i_k}^{j_k} \in \mathcal{B}_\ell^{j_k}(\Xi_{\ell,k}) \right\}.$$

We have used a bold and upright notation for the two-dimensional multi-indexes \mathbf{j} and \mathbf{i} , and will do so throughout the paper. To access their k -th entry we respectively write, as above, j_k and i_k , and we will denote the i_k -th knot of the level ℓ univariate knot vector $\Xi_{\ell,k}$ as $\xi_{i_k,\ell,k}$.

From this point forward, we will mainly refer to multi-variate basis functions either using the three indices \mathbf{j} , \mathbf{i} , and ℓ or omitting all of them whenever they are not necessary — unless otherwise specified. We are now capable of defining a set of finite element spaces such that the discrete complex they give is cohomologically equivalent to the continuous complex. The relevant spaces are

$$\mathbb{B}_\ell^0 := \mathbb{B}_\ell^{(0,0)}, \quad \mathbb{B}_\ell^1 := \mathbb{B}_\ell^{(1,0)} \times \mathbb{B}_\ell^{(0,1)}, \quad \mathbb{B}_\ell^2 := \mathbb{B}_\ell^{(1,1)},$$

and the discrete complex is naturally [10, 9]

$$\mathfrak{B}_h : \mathbb{B}_\ell^0 \xrightarrow{\mathbf{grad}} \mathbb{B}_\ell^1 \xrightarrow{\text{curl}} \mathbb{B}_\ell^2.$$

To help ease notation, we will use $\mathbf{0} = (0, 0)$ throughout the paper. Taking into account the way in which the **grad** and curl operators change the polynomial degree and regularity of functions it becomes clear that

$$\mathbf{grad}(\mathbb{B}_\ell^0) \subseteq \mathbb{B}_\ell^1, \quad \text{curl}(\mathbb{B}_\ell^1) \subseteq \mathbb{B}_\ell^2.$$

Finally, we also define the tensor-product mesh \mathcal{Q}_ℓ induced by the two sets of intervals $\mathcal{I}_{(\ell,1)}$ and $\mathcal{I}_{(\ell,2)}$, corresponding to $\Xi_{\ell,1}$ and $\Xi_{\ell,2}$, respectively. We define the mesh of level ℓ as

$$\mathcal{Q}_\ell = \{I_1 \times I_2 : I_1 \in \mathcal{I}_{(\ell,1)}, I_2 \in \mathcal{I}_{(\ell,2)}\}.$$

3.3. Hierarchical B-splines

With all the single-level tensor-product spline spaces from Section 3.2 in hand, we will construct a hierarchical B-spline space. We start by defining a set of nested domains and function spaces defined on them, assigning each domain and corresponding space to a specific refinement level. For the spaces, we require that $\mathbb{B}_0^{\mathbf{j}} \subseteq \mathbb{B}_1^{\mathbf{j}} \subseteq \dots \subseteq \mathbb{B}_L^{\mathbf{j}}$ for all valid \mathbf{j} . Lastly, our nested set of closed domains $\Omega_\ell \subset \mathbb{R}^2$ need to satisfy

$$\Omega =: \Omega_0 \supseteq \Omega_1 \supseteq \dots \supseteq \Omega_L \supseteq \Omega_{L+1} := \emptyset.$$

Furthermore, we also introduce the following assumption on how the subdomains that determine the mesh can be chosen.

Assumption 3.1. *We assume that $\Omega_{\ell+1}$ is given as the union of supports of B-splines in \mathcal{B}_ℓ^0 , that is*

$$\Omega_{\ell+1} := \bigcup_{B \in \tilde{\mathcal{B}}_\ell^0} \overline{\text{supp}(B)}, \quad \ell = \{0, \dots, L-1\},$$

where $\tilde{\mathcal{B}}_\ell^0 \subseteq \mathcal{B}_\ell^0$ is some set of level ℓ B-splines.

This leads us to defining a hierarchical mesh, \mathcal{Q} , as

$$\mathcal{Q} := \bigcup_{\ell \in \{0, \dots, L\}} \{Q \in \mathcal{Q}_\ell : Q \subseteq \Omega_\ell \wedge Q \not\subseteq \Omega_{\ell+1}\}.$$

As a consequence of Assumption 3.1, all elements of \mathcal{Q} are pairwise disjoint and $\bigcup_{Q \in \mathcal{Q}} \overline{Q} = \Omega$. Then, a standard way of selecting a basis $\mathcal{H}_L^{\mathbf{j}}$ for hierarchical B-spline spaces uses the following algorithm [22, 11]:

1. $\mathcal{H}_0^{\mathbf{j}} := \mathcal{B}_0^{\mathbf{j}}$.
2. For $\ell = 0, \dots, L-1$, let $\mathcal{H}_{\ell+1}^{\mathbf{j}} := \mathcal{H}_{\ell+1,A}^{\mathbf{j}} \cup \mathcal{H}_{\ell+1,B}^{\mathbf{j}}$, where

$$\begin{aligned} \mathcal{H}_{\ell+1,A}^{\mathbf{j}} &:= \left\{ B \in \mathcal{H}_\ell^{\mathbf{j}} : \text{supp}(B) \not\subseteq \Omega_{\ell+1} \right\}, \\ \mathcal{H}_{\ell+1,B}^{\mathbf{j}} &:= \left\{ B \in \mathcal{B}_{\ell+1}^{\mathbf{j}} : \text{supp}(B) \subseteq \Omega_{\ell+1} \right\}. \end{aligned}$$

We then set $\mathbb{H}_\ell^{\mathbf{j}} := \text{span}(\mathcal{H}_\ell^{\mathbf{j}})$, for any level $0 \leq \ell \leq L$. The corresponding hierarchical spaces are, then,

$$\mathbb{H}_\ell^0 := \mathbb{H}_\ell^{(0,0)}, \quad \mathbb{H}_\ell^1 := \mathbb{H}_\ell^{(1,0)} \times \mathbb{H}_\ell^{(0,1)}, \quad \mathbb{H}_\ell^2 := \mathbb{H}_\ell^{(1,1)},$$

and, for each $\ell = 0, \dots, L$, the hierarchical complex is

$$\mathfrak{H}_h : \mathbb{H}_\ell^0 \xrightarrow{\text{grad}} \mathbb{H}_\ell^1 \xrightarrow{\text{curl}} \mathbb{H}_\ell^2. \quad (2)$$

Remark 3.1. *Under Assumption 3.1, the three spaces in the complex (2) are associated to the same hierarchical mesh.*

The basis just defined above for hierarchical spaces can be slightly altered to preserve partition of unity and to reduce the support of the basis functions, through a procedure called truncation. For this, we introduce the higher-level representation of B-splines. Namely, given $B_{\mathbf{i},\ell}^{\mathbf{j}} \in \mathcal{B}_\ell^{\mathbf{j}}$, it is possible to write the basis function as

$$B_{\mathbf{i},\ell}^{\mathbf{j}} \equiv \sum_{B \in \mathcal{B}_{\ell+1}^{\mathbf{j}}} c_B^{\ell,\ell+1}(B_{\mathbf{i},\ell}^{\mathbf{j}})B, \quad c_B^{\ell,\ell+1}(B_{\mathbf{i},\ell}^{\mathbf{j}}) \in \mathbb{R}. \quad (3)$$

Using this property, we can then define the truncation operator at level $\ell+1$ as in [22]

$$\text{trunc}^{\ell+1}(B_{\mathbf{i},\ell}^{\mathbf{j}}) := \sum_{\substack{B \in \mathcal{B}_{\ell+1}^{\mathbf{j}} \\ \text{supp}(B) \not\subseteq \Omega_{\ell+1}}} c_B^{\ell,\ell+1}(B_{\mathbf{i},\ell}^{\mathbf{j}})B. \quad (4)$$

The truncation operation described above is linear and, in particular, can be written as a matrix multiplication; see [18] for more details.

Using this, the new truncated hierarchical basis is given by

1. $\mathcal{T}_0^j := \mathcal{B}_0^j$.
2. For $\ell = 0, \dots, L-1$, let $\mathcal{T}_{\ell+1}^j := \mathcal{T}_{\ell+1,A}^j \cup \mathcal{H}_{\ell+1,B}^j$, where

$$\mathcal{T}_{\ell+1,A}^j := \left\{ \text{trunc}^{\ell+1}(B) : B \in \mathcal{T}_\ell^j \wedge \text{supp}(B) \not\subseteq \Omega_{\ell+1} \right\}.$$

It is possible to show that $\text{span}(\mathcal{T}_\ell^j) = \text{span}(\mathcal{H}_\ell^j) = \mathbb{H}_\ell^j$ for all levels $\ell = 0, \dots, L$. While the two bases span the same space [22], the truncated basis is preferable in some instances due to the better matrix conditioning achieved with this basis and the recovery of the convex partition of unity property of tensor-product B-splines.

We will also define the notion of mother of a truncated B-spline [23]. Given a truncated basis function $T_{i,\ell}^j \in \mathcal{T}_\ell^j$, we say that $B_{i,\ell}^j$ is the mother of $T_{i,\ell}^j$ if

$$T_{i,\ell}^j = \text{trunc}^L \left(\dots \left(\text{trunc}^{\ell+1} \left(B_{i,\ell}^j \right) \right) \right),$$

and we denote this relationship as $\text{mot}(T_{i,\ell}^j) := B_{i,\ell}^j$.

We mentioned before how spurious harmonic forms can be introduced for arbitrary refinement domains. The reason for this can be understood by carefully considering the construction of the hierarchical spaces. The way in which the selection mechanism of active and inactive basis functions in each level works can, in principle, lead to a discrete complex with different cohomology spaces than the original one. This can happen because the coarse basis functions we remove from one level and the finer basis functions we replace them with in the next level can span spaces with different topological properties. See [32, Fig. 7] and [20, Fig. 13], and the surrounding discussions, for some illuminating examples of this phenomenon.

4. Admissibility

In adaptive methods for hierarchical splines, optimal order of convergence is proved by using the property of admissibility, which limits the difference of level between interacting functions [12, 13].

Definition 4.1. *We say that \mathbb{H}_L^j , $j \in \{0, 1, 2\}$, is \mathcal{H} - or \mathcal{T} -admissible of class m if on any element $Q \in \mathcal{Q}$, the non-vanishing basis functions in \mathcal{H}_L^j or \mathcal{T}_L^j , respectively, belong to at most m successive levels.*

By extension, we say that the hierarchical complex (2) is \mathcal{H} - or \mathcal{T} -admissible of class m if the corresponding previous condition holds for every $j \in \{0, 1, 2\}$.

The following definition relates a basis function with the ones involved when computing the differential operators. We also introduce a result which relates their support after truncation, that we will use in the proofs of admissibility. From now on, we will use δ_k to denote the two-dimensional index with value 1 at position k , and 0 in the other position.

Definition 4.2. *Let $B_{i,\ell}^j \in \mathcal{B}_\ell^j$ and $\mathbf{j}' - \mathbf{j} = \delta_k$ for some $k \in \{1, 2\}$. We say that $B_{i',\ell}^{\mathbf{j}'}$ is a k -derivation of $B_{i,\ell}^j$ if $\mathbf{i}' - \mathbf{i} = c\delta_k$, with $c \in \{0, 1\}$. Correspondingly, we say that $B_{i,\ell}^j$ is a k -integration of $B_{i',\ell}^{\mathbf{j}'}$.*

Proposition 4.1. *Let $T_{i,\ell}^j \in \mathcal{T}_\ell^j$ and $B_{i,\ell}^j = \text{mot}(T_{i,\ell}^j)$. Also, let $B_{i',\ell}^{\mathbf{j}'}$ be a k -derivation of $B_{i,\ell}^j$ for some $k \in \{1, 2\}$ and $T_{i',\ell}^{\mathbf{j}'} = \text{trunc}^L \left(\dots \left(\text{trunc}^{\ell+1} \left(B_{i',\ell}^{\mathbf{j}'} \right) \right) \right)$. Then, it holds that*

$$\text{supp}(T_{i,\ell}^j) \supseteq \text{supp}(T_{i',\ell}^{\mathbf{j}'}).$$

Proof. By definition, $\mathbf{i}' - \mathbf{i} = c\delta_k$, with $c \in \{0, 1\}$, for some $k \in \{1, 2\}$. Let us consider an active element $Q \in \mathcal{Q} \cap \mathcal{Q}_{\tilde{\ell}}$, with $\tilde{\ell} > \ell$, where $T_{\mathbf{i}, \ell}^{\mathbf{j}}$ is truncated, in the sense that it vanishes on Q . Also, let $\mathcal{R}_{Q, \tilde{\ell}}^{\mathbf{j}}$ denote the smallest subset of $\mathcal{B}_{\tilde{\ell}}^{\mathbf{j}}$ that can be linearly combined to represent $B_{\mathbf{i}, \ell}^{\mathbf{j}}$ on Q . Since $T_{\mathbf{i}, \ell}^{\mathbf{j}}$ vanishes on Q , we know that the support of B-splines in $\mathcal{R}_{Q, \tilde{\ell}}^{\mathbf{j}}$ is contained in $\Omega_{\tilde{\ell}}$. Moreover, we denote by $\mathcal{G}_{Q, \tilde{\ell}}^{\mathbf{j}'}$ the set of all k -derivations of B-splines in $\mathcal{R}_{Q, \tilde{\ell}}^{\mathbf{j}}$. Since all B-splines in $\mathcal{R}_{Q, \tilde{\ell}}^{\mathbf{j}}$ are supported on $\Omega_{\tilde{\ell}}$, all B-splines in $\mathcal{G}_{Q, \tilde{\ell}}^{\mathbf{j}'}$ must also be supported on $\Omega_{\tilde{\ell}}$.

Next, let $\mathcal{R}_{Q, \tilde{\ell}}^{\mathbf{j}'}$ be the smallest subset of $\mathcal{B}_{\tilde{\ell}}^{\mathbf{j}'}$ that can be linearly combined to represent $B_{\mathbf{i}', \ell}^{\mathbf{j}'}$ on Q . We must have $\mathcal{R}_{Q, \tilde{\ell}}^{\mathbf{j}'} \subseteq \mathcal{G}_{Q, \tilde{\ell}}^{\mathbf{j}'}$, because $B_{\mathbf{i}', \ell}^{\mathbf{j}'}$ is just one of the k -derivations of $B_{\mathbf{i}, \ell}^{\mathbf{j}}$. Thus, every B-spline in $\mathcal{R}_{Q, \tilde{\ell}}^{\mathbf{j}'}$ is supported on $\Omega_{\tilde{\ell}}$, and $T_{\mathbf{i}', \ell}^{\mathbf{j}'}$ must vanish on Q . \square

Lemma 4.2. *Under Assumption 3.1, if \mathbb{H}_L^0 is \mathcal{H} -admissible of class m so is \mathbb{H}_L^j for every $j \in \{1, 2\}$.*

Proof. Let us suppose that some $\mathbb{H}_L^{j'}$, with $j' \in \{1, 2\}$, is not \mathcal{H} -admissible of class m . In particular, this means that for some elements $Q \in \mathcal{Q} \cap \mathcal{Q}_{\ell}$ and $\tilde{Q} \in \mathcal{Q} \cap \mathcal{Q}_{\tilde{\ell}}$, with $\ell, \tilde{\ell} \in \{0, 1, \dots, L\}$ and $\tilde{\ell} > \ell + m - 1$, we have at least one active B-spline $B_{\mathbf{i}', \ell}^{\mathbf{j}'} \in \mathcal{H}_L^{\mathbf{j}'} \cap \mathcal{B}_{\ell}^{\mathbf{j}'}$, with $|\mathbf{j}'| = j'$, such that

$$\text{supp}(B_{\mathbf{i}', \ell}^{\mathbf{j}'}) \cap Q \neq \emptyset \wedge \text{supp}(B_{\mathbf{i}', \ell}^{\mathbf{j}'}) \cap \tilde{Q} \neq \emptyset, \quad (5)$$

and since the function is active we know that $\text{supp}(B_{\mathbf{i}', \ell}^{\mathbf{j}'}) \not\subseteq \Omega_{\ell+1}$. We will show that this implies the existence of a B-spline in \mathcal{H}_L^0 which contains both Q_{ℓ} and $Q_{\tilde{\ell}}$ in its support, thus contradicting the assumption on \mathbb{H}_L^0 .

We start by observing that we can find various B-splines such that the following chained containment holds,

$$\text{supp}(B_{\mathbf{i}, \ell}^0) \supseteq \dots \supseteq \text{supp}(B_{\mathbf{i}, \ell}^{\mathbf{j}}) \supseteq \text{supp}(B_{\mathbf{i}', \ell}^{\mathbf{j}'}),$$

and where each B-spline is a k -integration of the one to its right — possibly with different values for each k . Also, we can find another chained containment of B-splines for levels below ℓ ,

$$\text{supp}(B_{\mathbf{i}_0, 0}^0) \supseteq \dots \supseteq \text{supp}(B_{\mathbf{i}_{\ell-1}, \ell-1}^0) \supseteq \text{supp}(B_{\mathbf{i}, \ell}^0). \quad (6)$$

We know that none of the B-splines in (6) can be active, because their supports contain the support of $B_{\mathbf{i}', \ell}^{\mathbf{j}'}$, and this would lead to a contradiction on the admissibility class of \mathbb{H}_L^0 due to (5) and Assumption 3.1. However, $\text{supp}(B_{\mathbf{i}, \ell}^{\mathbf{j}'}) \not\subseteq \Omega_{\ell+1}$, which implies the same for all the functions in the sequence (6). Therefore, at least one of those functions must be active, which leads to a contradiction. \square

Lemma 4.3. *Under Assumption 3.1, if \mathbb{H}_L^0 is \mathcal{T} -admissible of class m so is \mathbb{H}_L^j for every $j \in \{1, 2\}$.*

Proof. Let us suppose that some $\mathbb{H}_L^{j'}$, with $j' \in \{1, 2\}$, is not \mathcal{T} -admissible of class m . In particular, this means that for some elements $Q \in \mathcal{Q} \cap \mathcal{Q}_{\ell}$ and $\tilde{Q} \in \mathcal{Q} \cap \mathcal{Q}_{\tilde{\ell}}$, with $\ell, \tilde{\ell} \in \{0, 1, \dots, L\}$ and $\tilde{\ell} > \ell + m - 1$, we have at least one active level ℓ truncated B-spline $T_{\mathbf{i}', \ell}^{\mathbf{j}'} \in \mathcal{T}_L^{\mathbf{j}'}$, with $|\mathbf{j}'| = j'$, such that

$$\text{supp}(T_{\mathbf{i}', \ell}^{\mathbf{j}'}) \cap Q \neq \emptyset \wedge \text{supp}(T_{\mathbf{i}', \ell}^{\mathbf{j}'}) \cap \tilde{Q} \neq \emptyset. \quad (7)$$

We will show that this implies the existence of a basis function in \mathcal{T}_L^0 which contains both Q_{ℓ} and $Q_{\tilde{\ell}}$ in its support, thus contradicting the assumption on \mathbb{H}_L^0 .

We start by observing that we can use Proposition 4.1, to find basis functions such that the following chained containment holds,

$$\text{supp}(T_{\mathbf{i}, \ell}^0) \supseteq \dots \supseteq \text{supp}(T_{\mathbf{i}, \ell}^{\mathbf{j}}) \supseteq \text{supp}(T_{\mathbf{i}', \ell}^{\mathbf{j}'}),$$

and where each mother B-spline is a k -integration of the one to its right — possibly with different values for each k .

It is true that $T_{\mathbf{i}_\ell, \ell}^{\mathbf{0}}$ can't be active, since this would violate the assumption on $\mathbb{H}_L^{\mathbf{0}}$ due to (7) and Assumption 3.1. Therefore, because the support of $T_{\mathbf{i}_\ell, \ell}^{\mathbf{0}}$ contains Q_ℓ we know that $\text{supp}(T_{\mathbf{i}_\ell, \ell}^{\mathbf{0}}) \not\subseteq \Omega_\ell$.

Let $T_{\mathbf{i}_{\ell-1}, \ell-1}^{\mathbf{0}}$ be such that $\text{mot}(T_{\mathbf{i}_\ell, \ell}^{\mathbf{0}})$ is used in the finer level representation of $\text{mot}(T_{\mathbf{i}_{\ell-1}, \ell-1}^{\mathbf{0}})$, as in (3). Then, because $\text{supp}(T_{\mathbf{i}_\ell, \ell}^{\mathbf{0}}) \not\subseteq \Omega_\ell$, we know that $T_{\mathbf{i}_\ell, \ell}^{\mathbf{0}}$ contributes to the representation of $T_{\mathbf{i}_{\ell-1}, \ell-1}^{\mathbf{0}}$ in (4). Again, if $T_{\mathbf{i}_{\ell-1}, \ell-1}^{\mathbf{0}}$ were active it would lead to a contradiction on the admissibility of $\mathbb{H}_L^{\mathbf{0}}$ because of (7) and Assumption 3.1. So, we know that $T_{\mathbf{i}_{\ell-1}, \ell-1}^{\mathbf{0}}$ is inactive and $\text{supp}(T_{\mathbf{i}_{\ell-1}, \ell-1}^{\mathbf{0}}) \not\subseteq \Omega_{\ell-1}$. We can repeat these steps recursively until we arrive at some $T_{\mathbf{i}_0, 0}^{\mathbf{0}}$ that is inactive because $\text{supp}(T_{\mathbf{i}_0, 0}^{\mathbf{0}}) \not\subseteq \Omega_0$, which leads to a contradiction since $\Omega_0 = \Omega$. \square

5. Exact Meshes

To begin this section, we introduce some notation to help the readability of the forthcoming proofs. First, we define the subset $\mathcal{B}_{\ell, \ell+1}^{\mathbf{0}} \subseteq \mathcal{B}_\ell^{\mathbf{0}}$ composed of B-splines in level ℓ whose support is contained in $\Omega_{\ell+1}$, i.e.,

$$\mathcal{B}_{\ell, \ell+1}^{\mathbf{0}} := \{B \in \mathcal{B}_\ell^{\mathbf{0}} : \text{supp}(B) \subseteq \Omega_{\ell+1}\} .$$

Second, we will simplify the notation of B-spline basis functions, and write $\beta_{\mathbf{i}} := B_{\mathbf{i}, \ell}^{\mathbf{0}}$, since all arguments in the proofs rely only on B-splines in the first space of the de Rham complex and two consecutive hierarchical levels.

We now move on to define precisely when a hierarchical refinement leads to an inexact complex, and how it can be altered by refining some additional functions to form an exact complex that satisfies the sufficient conditions in [32]. We first recall the definitions of chains and shortest chains from that paper, and we introduce some particular cases of shortest chains.

Definition 5.1 (Chain). *Let $\beta_{\mathbf{i}}, \beta_{\mathbf{j}} \in \mathcal{B}_{\ell, \ell+1}^{\mathbf{0}}$. We say that there is a chain between $\beta_{\mathbf{i}}$ and $\beta_{\mathbf{j}}$ if there exists $r \in \mathbb{Z}_{\geq 0}$ and B-splines $\beta_{\mathbf{t}_l} \in \mathcal{B}_{\ell, \ell+1}^{\mathbf{0}}$, $l = \{0, \dots, r\}$, such that $\beta_{\mathbf{i}} = \beta_{\mathbf{t}_0}, \beta_{\mathbf{j}} = \beta_{\mathbf{t}_r}$ and $|\mathbf{t}_l - \mathbf{t}_{l-1}| = 1$ for all $l \in \{1, \dots, r\}$. We will denote this chain by $C_{\mathbf{i}, \mathbf{j}} := \{\beta_{\mathbf{t}_l} \in \mathcal{B}_{\ell, \ell+1}^{\mathbf{0}} : l = 0, \dots, r\}$, and we will call r the length of the chain.*

Definition 5.2 (Shortest chain). *Let $\beta_{\mathbf{i}}, \beta_{\mathbf{j}} \in \mathcal{B}_{\ell, \ell+1}^{\mathbf{0}}$. A chain between $\beta_{\mathbf{i}}$ and $\beta_{\mathbf{j}}$, as in Definition 5.1, is said to be a shortest chain if we have $r = \sum_k |j_k - i_k|$.*

Definition 5.3 (Direction- k chain). *Let $\beta_{\mathbf{i}}, \beta_{\mathbf{j}} \in \mathcal{B}_{\ell, \ell+1}^{\mathbf{0}}$ and $k \in \{1, 2\}$ be such that $i_{k'} = j_{k'}$ for $k' \neq k$. We say that there is a direction- k chain between $\beta_{\mathbf{i}}$ and $\beta_{\mathbf{j}}$ if $\beta_{\mathbf{r}} \in \mathcal{B}_{\ell, \ell+1}^{\mathbf{0}}$ for every $\mathbf{r} \in \mathbb{N}^2$ such that*

$$\min\{i_k, j_k\} < r_k < \max\{i_k, j_k\} \wedge i_{k'} = r_{k'} = j_{k'} \text{ for } k' \neq k.$$

Definition 5.4 (L-chain). *Let $\beta_{\mathbf{i}}, \beta_{\mathbf{j}} \in \mathcal{B}_{\ell, \ell+1}^{\mathbf{0}}$. We say that there exists an L-chain between them if for some $\beta_{\mathbf{c}} \in \mathcal{B}_{\ell, \ell+1}^{\mathbf{0}}$ there exists a direction- k_1 chain, $C_{\mathbf{i}, \mathbf{c}}$, between $\beta_{\mathbf{i}}$ and $\beta_{\mathbf{c}}$ and a direction- k_2 chain, $C_{\mathbf{c}, \mathbf{j}}$, between $\beta_{\mathbf{c}}$ and $\beta_{\mathbf{j}}$, such that $k_1 \neq k_2$. The union of the chains $C_{\mathbf{i}, \mathbf{c}}$ and $C_{\mathbf{c}, \mathbf{j}}$ is called the L-chain between $\beta_{\mathbf{i}}$ and $\beta_{\mathbf{j}}$, and $\beta_{\mathbf{c}}$ is called its corner element.*

Lemma 5.1. *Let $\beta_{\mathbf{i}}, \beta_{\mathbf{j}} \in \mathcal{B}_{\ell, \ell+1}^{\mathbf{0}}$ have a direction- k chain $C_{\mathbf{i}, \mathbf{j}}$ between them. Then, $C_{\mathbf{i}, \mathbf{j}}$ is a shortest chain.*

Proof. Let $\Delta = \mathbf{j} - \mathbf{i}$ and assume w.l.o.g that $\Delta_k \geq 0$. Then, the direction- k chain $C_{\mathbf{i}, \mathbf{j}}$ is equal to

$$\{\beta_{\mathbf{i}}, \beta_{\mathbf{i}+\delta_k}, \beta_{\mathbf{i}+2\delta_k}, \dots, \beta_{\mathbf{j}}\} .$$

It is clear that this chain satisfies the conditions for being a shortest chain, since its length is $|\Delta| = j_k - i_k$. \square

Lemma 5.2. *Let $\beta_{\mathbf{i}}, \beta_{\mathbf{j}} \in \mathcal{B}_{\ell, \ell+1}^{\mathbf{0}}$. Then, any L-chain between them is a shortest chain.*

Proof. Assume without loss of generality that $j_k \geq i_k$, for $k = 1, 2$. Since the L-chain is the union of a direction-1 and direction-2 chain, it is easy to see that its length is $(j_1 - i_1) + (j_2 - i_2) = |\mathbf{j} - \mathbf{i}|$, and hence it is a shortest chain. \square

The following are two definitions and the main result from [32], that gives a sufficient condition for exactness.

Definition 5.5. Let $\beta_{\mathbf{i}}, \beta_{\mathbf{j}} \in \mathcal{B}_{\ell, \ell+1}^0$. We say that $\beta_{\mathbf{i}}$ and $\beta_{\mathbf{j}}$ share a minimal $(\ell + 1)$ -intersection if there exists some $k_0 \in \{1, 2\}$ and $(\xi_{t_1, \ell+1, 1}, \xi_{t_2, \ell+1, 2}) \in \Xi_{\ell+1, 1} \times \Xi_{\ell+1, 2}$ such that

$$\overline{\text{supp}(\beta_{\mathbf{i}})} \cap \overline{\text{supp}(\beta_{\mathbf{j}})} \supseteq \bigtimes_{k=1}^2 I_k ,$$

$$I_k := \begin{cases} (\xi_{t_k, \ell+1, k}, \xi_{t_k + p(\ell+1, k), \ell+1, k}) , & k \neq k_0 , \\ \{\xi_{t_k, \ell+1, k}\} , & k = k_0 . \end{cases}$$

Definition 5.6 (Problematic pairs and chains). Let $\beta_{\mathbf{i}}, \beta_{\mathbf{j}} \in \mathcal{B}_{\ell, \ell+1}^0$ share a minimal $(\ell + 1)$ -intersection. We say that the pair is problematic if there is no shortest chain between them. We also say that a chain is problematic with $\beta_{\mathbf{i}}$ if any spline in the chain is problematic with $\beta_{\mathbf{i}}$.

Theorem 5.3 ([32], Theorem 4.24). Let us assume that, for every $\beta_{\mathbf{i}}, \beta_{\mathbf{j}} \in \mathcal{B}_{\ell, \ell+1}^0$ sharing a minimal $(\ell + 1)$ -intersection, there exists a shortest chain $C_{\mathbf{i}, \mathbf{j}}$ between them, for $\ell = 0, \dots, L$. Then the hierarchical complex (2) is exact for $\ell = 0, \dots, L$.

To fix problematic pairs it is necessary to join them by a shortest chain of refined B-splines. However, additional refinement can lead to new problematic pairs that need to be checked and resolved recursively. The following results show that L-chains reduce the number of checks to be performed during this process.

Definition 5.7. Let $\beta_{\mathbf{i}} \in \mathcal{B}_{\ell, \ell+1}^0$ and $k \in \{1, 2\}$. We define the k -side configuration of $\beta_{\mathbf{i}}$ as

$$S_{\mathbf{i}, k} := \{ \beta_{\mathbf{t}} \in \mathcal{B}_{\ell}^0 : \mathbf{t} - \mathbf{i} = \pm \delta_k , \} .$$

Moreover, we say that $\beta_{\mathbf{i}} \in \mathcal{B}_{\ell, \ell+1}^0$ is resolved in direction k if $S_{\mathbf{i}, k} \subseteq \mathcal{B}_{\ell, \ell+1}^0$.

Lemma 5.4 (Problematic sides). Let $\beta_{\mathbf{i}}, \beta_{\mathbf{j}} \in \mathcal{B}_{\ell, \ell+1}^0$ be a problematic pair, and $\beta_{\mathbf{i}}$ be resolved in direction $k \in \{1, 2\}$. Then, there must be some $\beta_{\mathbf{t}} \in S_{\mathbf{i}, k}$ that is problematic with $\beta_{\mathbf{j}}$, and $|t_k - j_k| < |i_k - j_k|$.

Proof. Since $\beta_{\mathbf{i}}$ is resolved in direction k , by definition there exists $\beta_{\mathbf{t}} \in S_{\mathbf{i}, k}$ such that $|t_k - j_k| < |i_k - j_k|$. This implies that $\overline{\text{supp}(\beta_{\mathbf{i}})} \cap \overline{\text{supp}(\beta_{\mathbf{j}})} \subseteq \overline{\text{supp}(\beta_{\mathbf{t}})} \cap \overline{\text{supp}(\beta_{\mathbf{j}})}$, which in turn means that there is a minimal $(\ell + 1)$ -intersection between $\beta_{\mathbf{t}}$ and $\beta_{\mathbf{j}}$. Since a shortest chain between $\beta_{\mathbf{t}}$ and $\beta_{\mathbf{j}}$ would result in a shortest chain between $\beta_{\mathbf{i}}$ and $\beta_{\mathbf{j}}$, and hence a contradiction, the pair $\beta_{\mathbf{t}}, \beta_{\mathbf{j}}$ must be problematic. \square

Lemma 5.5 (Problematic chain in 2D). Let $\beta_{\mathbf{i}}, \beta_{\mathbf{j}}, \beta_{\mathbf{c}} \in \mathcal{B}_{\ell, \ell+1}^0$ be such that there exists an L-chain $C_{\mathbf{i}, \mathbf{j}}$ between $\beta_{\mathbf{i}}$ and $\beta_{\mathbf{j}}$, with corner element $\beta_{\mathbf{c}}$. If $\beta_{\mathbf{i}}$ is problematic with $C_{\mathbf{i}, \mathbf{j}}$, then it must be problematic with at least one of $\beta_{\mathbf{i}}, \beta_{\mathbf{j}}$ and $\beta_{\mathbf{c}}$.

Proof. Suppose $\beta_{\mathbf{i}}$ is problematic with some $\beta_{\mathbf{t}} \in C_{\mathbf{i}, \mathbf{j}}$. If $\beta_{\mathbf{t}} \in \{\beta_{\mathbf{i}}, \beta_{\mathbf{j}}, \beta_{\mathbf{c}}\}$ the proof is trivial, so, consider $\beta_{\mathbf{t}} \in C_{\mathbf{i}, \mathbf{j}} \setminus \{\beta_{\mathbf{i}}, \beta_{\mathbf{j}}, \beta_{\mathbf{c}}\}$. Then, since $\beta_{\mathbf{t}}$ will be resolved in some direction k , we can recursively apply Lemma 5.4 to prove that there exists $\beta_{\mathbf{v}} \in \{\beta_{\mathbf{i}}, \beta_{\mathbf{j}}, \beta_{\mathbf{c}}\}$ that is problematic with $\beta_{\mathbf{i}}$. \square

We now introduce the concept of an interaction box, and some related results that will help to simplify the search for shortest chains in the algorithms of Section 6.

Definition 5.8. Let $\beta_{\mathbf{i}} \in \mathcal{B}_{\ell, \ell+1}^0$. We define the interaction box $\square_{\mathbf{i}}$ of $\beta_{\mathbf{i}}$ as the set of B-splines in $\mathcal{B}_{\ell, \ell+1}^0$ that are at a maximum distance of $p(\ell, k) + 1$ knot indices, in each dimension. In other words,

$$\square_{\mathbf{i}} := \{ \beta_{\mathbf{j}} \in \mathcal{B}_{\ell, \ell+1}^0 : |i_k - j_k| \leq p(\ell, k) + 1, \text{ for } k = 1, 2 \} .$$

To refer to the intersection of two interaction boxes \square_i and \mathbf{j} we will write $\square_{i,\mathbf{j}} := \square_i \cap \square_{\mathbf{j}}$.

Lemma 5.6. *Let $\beta_i, \beta_j \in \mathcal{B}_{\ell, \ell+1}^0$. If $C_{i,\mathbf{j}}$ is a chain contained in $\square_{i,\mathbf{j}}$, then there exists a shortest chain between β_i and β_j .*

Proof. If a subset of $C_{i,\mathbf{j}}$ is a shortest chain then we are done. Suppose then that no subset of $C_{i,\mathbf{j}}$ is a shortest chain and assume, w.l.o.g, that $i_k < j_k$, for $k = 1, 2$. By the chain not being a shortest chain, we know that there must exist at least one pair, $\beta_1, \beta_t \in C_{i,\mathbf{j}} \cap \square_{i,\mathbf{j}}$, with a “kink”. By this, we mean that there exists $k \in \{1, 2\}$ such that $l_k = t_k$ but the corresponding direction- k' chain $C_{1,t}$, $k' \in \{1, 2\} \setminus k$, is not a subset of $C_{i,\mathbf{j}}$. However, since β_1 and β_t are both in $\square_{i,\mathbf{j}}$, their supports have a non-empty intersection, which implies that $\text{supp}(\beta_{\mathbf{r}}) \subseteq \overline{\text{supp}(\beta_1)} \cup \overline{\text{supp}(\beta_t)} \subseteq \Omega_{\ell+1}$ for all $\mathbf{r} \in \mathbb{N}^2$ such that

$$l_k = r_k = t_k \wedge \min(l_{k'}, t_{k'}) < r_{k'} < \max(l_{k'}, t_{k'}) .$$

Hence, all the B-splines in $C_{1,t}$ belong to $\mathcal{B}_{\ell, \ell+1}^0$, and as a consequence to $\square_{i,\mathbf{j}}$, and we can use them to remove the “kink” between β_1 and β_t to obtain a new chain $\tilde{C}_{i,\mathbf{j}}$ with a smaller length. Repeating the procedure for every such “kink” will yield a shortest chain between β_i and β_j . \square

Lemma 5.7. *Let $\beta_i, \beta_j \in \mathcal{B}_{\ell, \ell+1}^0$ share a minimal $(\ell + 1)$ -intersection and have an L-chain in $C_{i,\mathbf{j}}$ between them. Moreover, let β_1 share a minimal $(\ell + 1)$ -intersection with some $\beta_t \in C_{i,\mathbf{j}}$ and such that there is an L-chain $C_{1,t}$. Then, there are no problematic pairs between $C_{i,\mathbf{j}}$ and $C_{1,t}$.*

Proof. We will prove the result directly, by showing that there is a shortest chain between any pair of B-splines, one in each L-chain, that share a minimal $(\ell + 1)$ -intersection.

As such, suppose that $\beta_{\mathbf{p}} \in C_{i,\mathbf{j}}$ and $\beta_{\mathbf{p}'}$ in $C_{1,t}$ share a minimal $(\ell + 1)$ -intersection. Since β_i and β_j share a minimal $(\ell + 1)$ -intersection, the same is true for any other pair of B-splines in $C_{i,\mathbf{j}}$, and in particular for $\beta_{\mathbf{p}}$ and β_t . Analogously, $\beta_{\mathbf{p}'}$ and β_t must also share a minimal $(\ell + 1)$ -intersection. Hence, we can conclude that $\beta_t \in \square_{\mathbf{p}, \mathbf{p}'}$.

Using the definition of L-chains, it is clear that we can find subsets of $C_{i,\mathbf{j}}$ and $C_{1,t}$, contained in $\square_{\mathbf{p}, \mathbf{p}'}$, that are chains between β_t and $\beta_{\mathbf{p}}$ and β_t and $\beta_{\mathbf{p}'}$, respectively. Invoking Lemma 5.6, we reason that there is a shortest chain between $\beta_{\mathbf{p}}$ and $\beta_{\mathbf{p}'}$, thus finishing the proof. \square

Remark 5.1. *Let $\beta_i, \beta_j \in \mathcal{B}_{\ell, \ell+1}^0$ be a problematic pair. There are two possible L-chains that can be constructed between the pair — depending on the corner element chosen. It is always preferable to choose the L-chain that leads to the highest number of resolved B-splines, as this reduces the necessary checks for new problematic pairs.*

6. Algorithms

In this section, we will describe a set of algorithms that can be easily incorporated into standard numerical solvers, and that ensure that the resulting discrete de Rham complex remains exact after local refinement.

The main algorithm is Algorithm 1, which takes as input a hierarchical space, described by its basis \mathcal{T}_L^0 , and a set of elements marked for refinement, and returns an updated basis that leads to an exact complex. The algorithm is subdivided into five steps, the first three corresponding to Algorithms 2 to 4.

The first step is to obtain the basis functions that need to be checked for problematic pairs. Here, we compute the basis functions in $\mathcal{B}_{\ell, \ell+1}^0$ and then use Lemma 5.4 to discard basis functions that are resolved in some direction, to remove unnecessary computations. Then, we loop over all unordered pairs of relevant basis functions and use Algorithms 3 and 4 to check if the pair is problematic, comprising steps two and three. See Fig. 1 for an illustration.

Algorithm 3 performs the check for a minimal $(\ell + 1)$ -intersection between the pair using Definition 5.5. It first calls the method `get_support_per_dim`, that computes the breakpoint-interval indices of the intervals where a basis function is supported, in each dimension, as defined in (1); concretely, if the support of B in dimension k contains only the intervals $(\zeta_i, \zeta_{i+1}), \dots, (\zeta_j, \zeta_{j+1})$, for some i, j , then `get_support_per_dim`

would return the integers $\{i, \dots, j+1\}$. Then, the algorithm computes the intersection of the supports of the pair of basis functions, and by working with the integer indices of the intervals the subsequent computations are cheaper than if using real values. Another method used in this algorithm that should be implemented is `get_contained_indices`, which returns the biggest subset of $\Xi_{(\ell+1,k)}$ contained in the intersection of the pair's supports, for a given dimension k and level ℓ .

The Algorithm 4 used in the third step assumes that the given pair of basis functions shares a minimal $(\ell+1)$ -intersection, since this is the appropriate case for Algorithm 1, and it makes the check of a direction- k chain between the pair trivial. If no such chain exists, we then construct the interaction box, as in Definition 5.8, and check if there is a shortest chain between the pair using Lemma 5.6. To do this, we chose to implement the interaction box as a graph — in this case, a subgraph of a lattice graph — and then use a standard algorithm to check if a path exists between nodes on a graph, named as `has_chain` in the algorithm. Packages that perform these operations are commonplace and should be available in most programming languages.

We reach the fourth step when a pair of B-splines is problematic. In this case, we use the method `get_lchain_indices` to select what L-chain should be added, according to Remark 5.1, and return all the indices of the basis functions in the L-chain and its corner function. This information is used to update the basis functions and marked elements used in the next iteration of checking for problematic pairs.

The last step consists of computing all the new pairs that will need to be checked, taking into account those that were already fixed with the added L-chains, and updating the hierarchical basis accordingly.

Finally, steps two to five are repeated until there are no more problematic pairs in the hierarchical basis.

Remark 6.1. *Algorithm 1 can be adapted to enforce an admissible \mathbb{H}_L^0 with few alterations. Notice that the addition of L-chains only affects the elements marked for refinement at a given level ℓ , and the imposition of admissibility the elements at levels below ℓ . Therefore, we can reverse the outermost loop in the algorithm, starting from the finer level and going down to the coarsest level, and perform the admissibility imposition after all the problematic pairs at a given level have been fixed. This way, we ensure that any possible problematic pair introduced by the addition of admissibility will still be fixed in the following iterations.*

Algorithm 1 Exact mesh refinement.

Require: \mathcal{T}_L^0 , a set of marked elements to refine per level `marked_els`

Ensure: Updated truncated hierarchical basis \mathcal{T}_L^0 with no problematic intersections

```
1: for all  $\ell$  in  $\{0, \dots, L-1\}$  do
2:   unchecked_pairs  $\leftarrow$  initiate_unchecked_pairs( $\mathcal{T}_L^0, \ell, \text{marked\_els}$ )
3:   checked_pairs  $\leftarrow \emptyset$ 
4:   problematic_mesh  $\leftarrow$  true
5:   while problematic_mesh do
6:     problematic_mesh  $\leftarrow$  false
7:     for all pair in unchecked_pairs do
8:       has_min_intersec  $\leftarrow$  has_minimal_intersection( $\mathcal{T}_L^0, \ell, \text{pair}$ )
9:       if  $\neg$ has_min_intersec then
10:        skip iteration
11:       has_no_chain  $\leftarrow$   $\neg$ has_shortest_chain( $\mathcal{T}_L^0, \ell, \text{pair}$ )
12:       if has_no_chain then
13:         lchain, corner_func  $\leftarrow$  get_lchain_indices( $\mathcal{T}_L^0, \ell, \text{pair}$ )
14:         unchecked_funcs  $\leftarrow$  unchecked_funcs  $\cup$  corner_func
15:         marked_els[ $\ell$ ]  $\leftarrow$  marked_els[ $\ell$ ]  $\cup$  get_support(lchain)
16:         problematic_mesh  $\leftarrow$  true
17:       checked_pairs  $\leftarrow$  checked_pairs  $\cup$  unchecked_pairs
18:       unchecked_pairs  $\leftarrow$  combinations(unchecked_funcs, 2)
19:       unchecked_pairs  $\leftarrow$  unchecked_pairs  $\setminus$  checked_pairs
20:        $\mathcal{T}_L^0 \leftarrow$  update_hierarchical_space( $\mathcal{T}_L^0, \text{marked\_els}$ )
21: return  $\mathcal{T}_L^0$ 
```

Algorithm 2 initiate_unchecked_pairs

Require: \mathcal{T}_L^0 , hierarchical level ℓ , set of marked elements to refine per level `marked_els`

Ensure: pairs of basis functions that might be problematic

```
1:  $\Omega_{\ell+1} \leftarrow \Omega_{\ell+1} \cup \text{marked\_els}$ 
2: supported_funcs  $\leftarrow \mathcal{B}_{\ell, \ell+1}^0$   $\triangleright$  As defined in Section 5.
3: unchecked_funcs  $\leftarrow \emptyset$ 
4: for all  $\beta_i \in$  supported_funcs do
5:   for all  $k$  in  $\{1, 2\}$  do
6:     if  $\beta_i$  is resolved in  $k$  then
7:       skip iteration  $\triangleright$  Using Lemma 5.4.
8:   unchecked_funcs  $\leftarrow$  unchecked_funcs  $\cup \beta_i$ 
9: unchecked_pairs  $\leftarrow$  combinations(unchecked_funcs, 2)
10: for all  $(\beta_i, \beta_j)$  in unchecked_pairs do
11:   if  $\text{supp}(\beta_i) \cap \text{marked\_els} == \emptyset$  and  $\text{supp}(\beta_j) \cap \text{marked\_els} == \emptyset$  then
12:     unchecked_pairs  $\leftarrow$  unchecked_pairs  $\setminus (\beta_i, \beta_j)$ 
13: return unchecked_pairs
```

Algorithm 3 `has_minimal_intersection` (Checks if there is a minimal $(\ell + 1)$ -intersection between a pair of B-splines.)

Require: \mathcal{T}_L^0 , pair = (β_i, β_j) , hierarchical level ℓ .

Ensure: Boolean indicating if the pair shares a minimal $(\ell + 1)$ -intersection.

```

1: supp_bi  $\leftarrow$  get_support_per_dim ( $\beta_i$ )
2: supp_bj  $\leftarrow$  get_support_per_dim ( $\beta_j$ )
3: for all  $k$  in  $\{1, 2\}$  do
4:   supp_intersection  $\leftarrow$  supp_bi[k]  $\cap$  supp_bj[k]
5:   if supp_intersection ==  $\emptyset$  then
6:      $\perp$  return false
7:    $I_k \leftarrow$  get_contained_indices(supp_intersection,  $\Xi_{(\ell+1,k)}$ )  $\triangleright$  At level  $\ell + 1$ .
8:   length_flag[k]  $\leftarrow$  length( $I_k$ ) >  $p_{(\ell+1,k)}$   $\triangleright$  Condition of Definition 5.5.
9: has_min_intersec  $\leftarrow$  any(length_flag) == true
10: return has_min_intersec

```

Algorithm 4 `has_shortest_chain` (Checks if a pair of B-splines that share a minimal $(\ell + 1)$ -intersection have a shortest chain between them.)

Require: \mathcal{T}_L^0 , pair = (β_i, β_j) , hierarchical level ℓ .

Ensure: Boolean indicating if there is a shortest chain between the pair of B-splines.

```

1: if any( $i - j$ ) == 0 then
2:    $\perp$  return true  $\triangleright$  There is a direction- $k$  chain.
3: inter_box  $\leftarrow$   $\square_{i,j}$   $\triangleright$  As in Definition 5.8.
4: if has_chain(inter_box,  $i$ ,  $j$ ) then
5:   return true  $\triangleright$  Using Lemma 5.6.
6: else
7:    $\perp$  return false

```

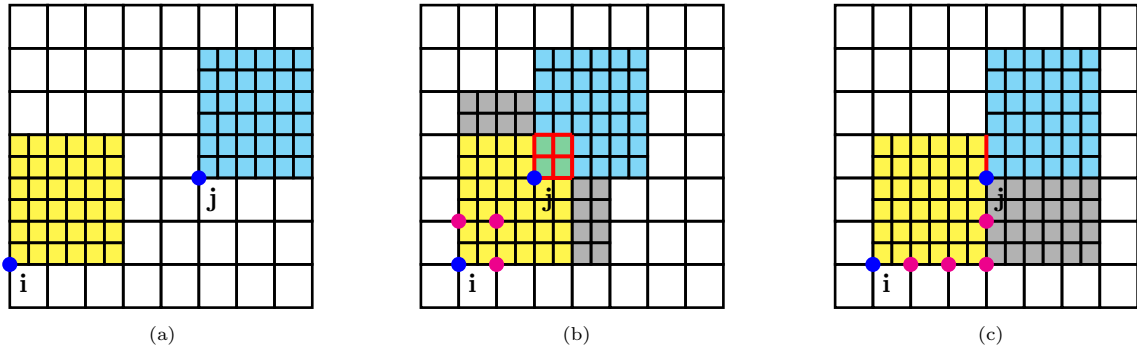


Figure 1: Illustration of Algorithms 3 and 4 for three different cases, all using $p_{(\ell,k)} = 2$ for all ℓ and k . In the left figure there is no problematic pair, in the centre figure there is a problematic pair and in the last figure there is a minimal $(\ell + 1)$ -intersection and a shortest chain, so the pair is not problematic. The union of all shaded cells represents $\Omega_{\ell+1}$, while the supports of β_i and β_j are coloured in yellow and cyan, respectively, and their intersection in green. Also, the possible I_k contained in the intersection of the supports of β_i and β_j , as in Definition 5.5, are highlighted in red. Finally, blue dots represent the indices i and j and magenta dots the indices of the other B-splines in $\mathcal{B}_{\ell,\ell+1}^0$.

Lemma 6.1. *Algorithm 1 always produces an exact mesh.*

Proof. The result follows as a consequence of Lemmas 5.2, 5.4 and 5.5. □

7. Numerical Results

In order to show that the theory holds numerically, we have devised some tests for the non-homogeneous vector Laplace problem and the Maxwell eigenvalue problem. We focus on these tests, which are formulated using vector fields, since the homogeneous boundary conditions that arise in the weak formulations of these problems, both essential and natural, imply the non-existence of harmonic scalar fields.

For all the ensuing examples, we chose to work with h -refinement for primarily two reasons. First, it makes for more visually compelling examples of what sorts of refinements are problematic or not. Second, using p -refinement precludes the use of maximally smooth B-splines, which is one of the major advantages of IGA. Despite this, all the results in Section 5 still hold for such refinement schemes.

7.1. Vector Laplace problem

Let the domain $\Omega \subseteq \mathbb{R}^2$ be the unit square $[0, 1]^2$. Since the domain is simply connected, the continuous de Rham complex has no harmonic vector fields, and as such, neither should our discretized complex. Considering the mixed weak formulation of the vector Laplace problem with natural, homogeneous boundary conditions, the relevant objects we wish to find are $\sigma \in H^1(\Omega)$ and $\mathbf{u} \in \mathbf{H}(\text{curl}; \Omega)$ such that

$$\begin{aligned} \langle \sigma, \tau \rangle - \langle \mathbf{u}, \mathbf{grad} \tau \rangle &= 0, & \forall \tau \in H^1(\Omega), \\ \langle \mathbf{grad} \sigma, \mathbf{v} \rangle + \langle \text{curl} \mathbf{u}, \text{curl} \mathbf{v} \rangle &= \langle \mathbf{f}, \mathbf{v} \rangle, & \forall \mathbf{v} \in \mathbf{H}(\text{curl}; \Omega). \end{aligned}$$

For the first test, we will take as the analytical solution

$$\mathbf{u}(x, y) = \begin{bmatrix} x(1-x) \\ 0 \end{bmatrix}. \quad (8)$$

We will try to solve the problem on two different meshes — one exact and the other not — just to illustrate the spurious results that can arise from refinement that does not respect the conditions for exactness. The two meshes are shown in Fig. 2. We will denote the computed solution using the Figs. 2a and 2b meshes as \mathbf{u}_h^a and \mathbf{u}_h^b , respectively.

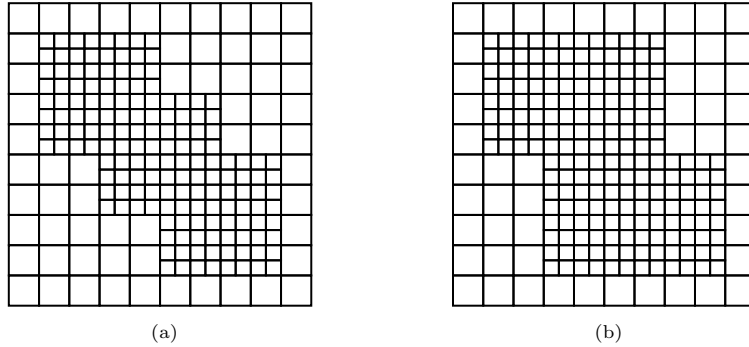


Figure 2: Two hierarchical meshes. The mesh in Fig. 2a has two problematic intersections while the one in Fig. 2b is the result of applying Algorithm 1 to the mesh in Fig. 2a and therefore has none.

The discrete version of the problem is then to find $\sigma_h \in \mathbb{T}_L^0$ and $\mathbf{u}_h \in \mathbb{T}_L^1$ such that

$$\begin{aligned} \langle \sigma_h, \tau \rangle - \langle \mathbf{u}_h, \mathbf{grad} \tau \rangle &= 0, & \forall \tau \in \mathbb{T}_L^0, \\ \langle \mathbf{grad} \sigma_h, \mathbf{v} \rangle + \langle \text{curl} \mathbf{u}_h, \text{curl} \mathbf{v} \rangle &= \langle \mathbf{f}, \mathbf{v} \rangle, & \forall \mathbf{v} \in \mathbb{T}_L^1, \end{aligned}$$

and $p_{(\ell, k)} = 3$ for all ℓ and k . It is easy to see that $u \subseteq \mathbb{T}_L^1$, and therefore we should be able to compute the solution exactly, up to machine precision, in the case of Fig. 2b. However, due to the problematic

intersections in Fig. 2a we expect to introduce spurious harmonic vector fields. This is evidenced after computing the corresponding L^2 -norm errors, as we get the values

$$\|\mathbf{u}_h^a - \mathbf{u}\| \approx 0.084037, \quad \|\mathbf{u}_h^b - \mathbf{u}\| \approx 4.946255 \times 10^{-16}.$$

The appearance of spurious harmonic vector fields introduced by the problematic intersections can also be seen in Fig. 3.

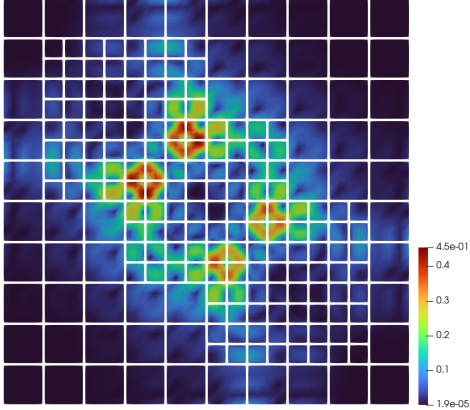


Figure 3: Plot of the magnitude of the vector field $\mathbf{u}_h^a - \mathbf{u}$, for \mathbf{u} in eq. (8), showcasing the spurious harmonic vector fields.

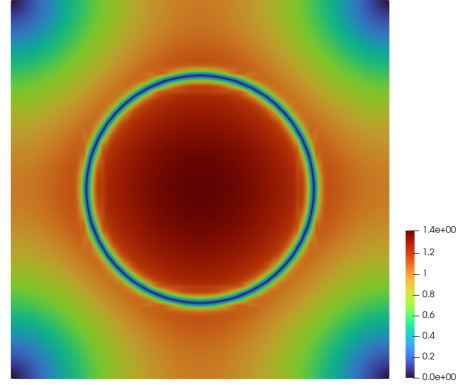


Figure 4: Magnitude of the analytical solution in eq. (9).

In the second test, the analytical solution is

$$\mathbf{u}(x, y) = \begin{bmatrix} \sin(\pi x)(1 - \tanh(100((x - 0.5)^2 + (y - 0.5)^2 - 0.3^2))) \\ \sin(\pi y)(1 - \tanh(100((x - 0.5)^2 + (y - 0.5)^2 - 0.3^2))) \end{bmatrix}. \quad (9)$$

To get a better sense of the circular feature present in the problem, we show a plot of the analytical solution in Fig. 4.

We will perform an adaptive refinement scheme, using the analytical solution to calculate the L^2 -error per element and a Dörfler parameter $\theta = 0.06$ to mark elements for refinement. This parameter determines the cut-off error from which elements are no longer refined. We refer the reader to [16, 13] for extra details.

The starting finite element space of $\mathcal{X}^{(0,0)}$, corresponding to a tensor product B-spline space, has polynomial degree $p_{(0,k)} = 3$ for both dimensions, and it will be kept as such for all further refinement levels. Figs. 5 and 6 demonstrate the difference between the adaptive refinement techniques both with and without the refinement scheme of Algorithm 1. There, it is easy to see the kind of behaviour that can arise when exact refinements are not considered during the refinement process.

7.2. Maxwell eigenvalue problem

Consider now the domain $\Omega \subseteq \mathbb{R}^2$ as the square $[0, \pi]^2$. In this case, problem in question is to find $\omega \in \mathbb{R}$ and $\mathbf{u} \in \mathring{\mathbf{H}}(\text{curl}; \Omega)$ such that

$$\langle \text{curl } \mathbf{u}, \text{curl } \mathbf{v} \rangle = \omega^2 \langle \mathbf{u}, \mathbf{v} \rangle, \quad \forall \mathbf{v} \in \mathring{\mathbf{H}}(\text{curl}; \Omega),$$

where

$$\mathring{\mathbf{H}}(\text{curl}; \Omega) := \{\mathbf{v} \in \mathbf{H}(\text{curl}; \Omega) : \mathbf{v} \times \mathbf{n} = 0 \text{ on } \partial\Omega\},$$

where \mathbf{n} is the outward unit normal to the boundary of Ω . It is well known that the eigenvalue solutions satisfy $\omega^2 = m^2 + n^2$ with $m, n \in \{0, 1, \dots\}$. Once again, no harmonic vector fields are expected due to

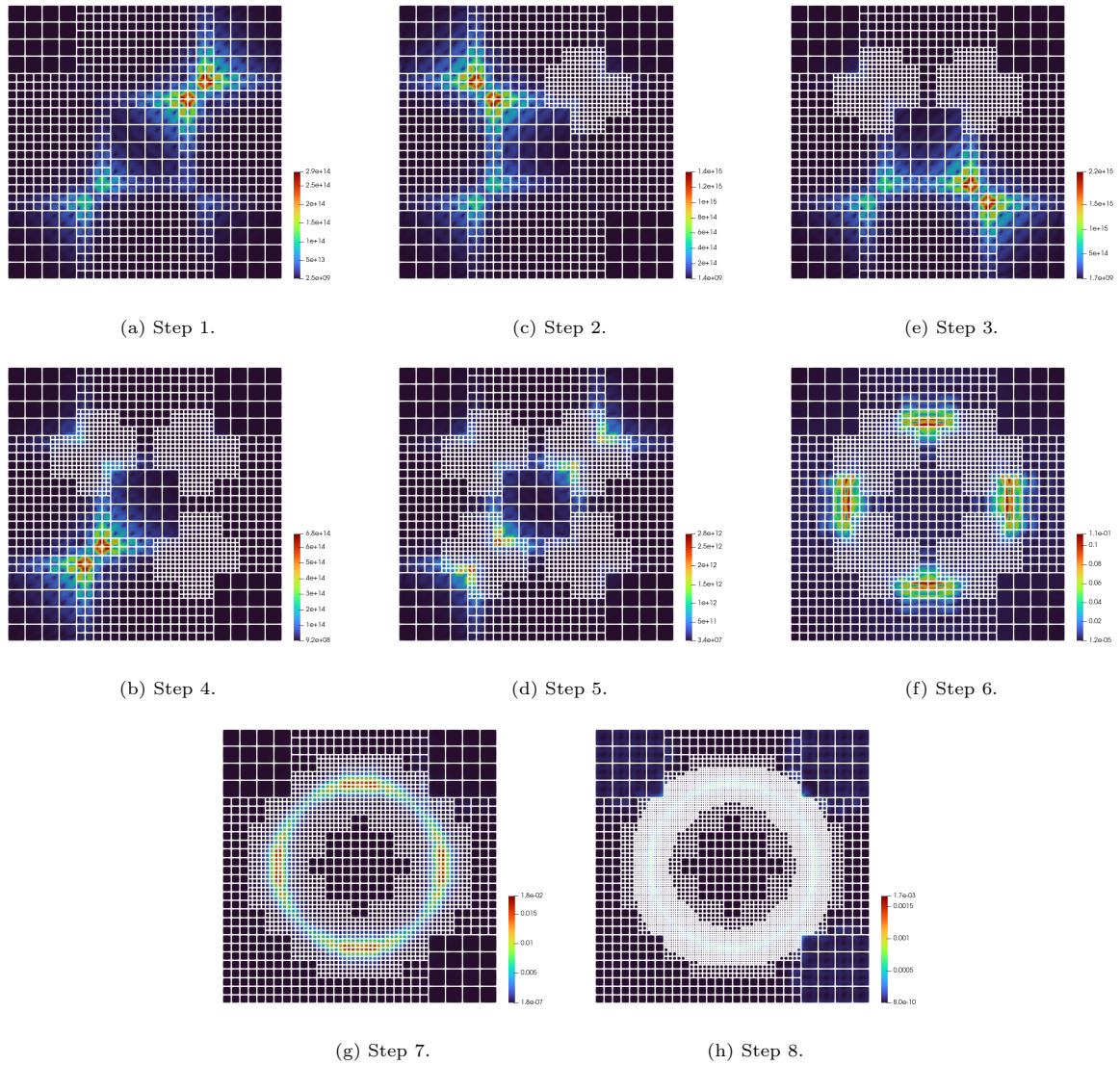


Figure 5: Adaptive refinement without Algorithm 1 for the vector Laplace problem with analytical solution (9). After the first refinement 4 problematic intersections are introduced. Moreover, each intersection is responsible for an error with a different order of magnitude than rest, making it hard to resolve this issue in a single step of the adaptive loop. As a consequence, 4 steps of the process are wasted refining these intersections until, by mere chance, this is fixed in Step 6.

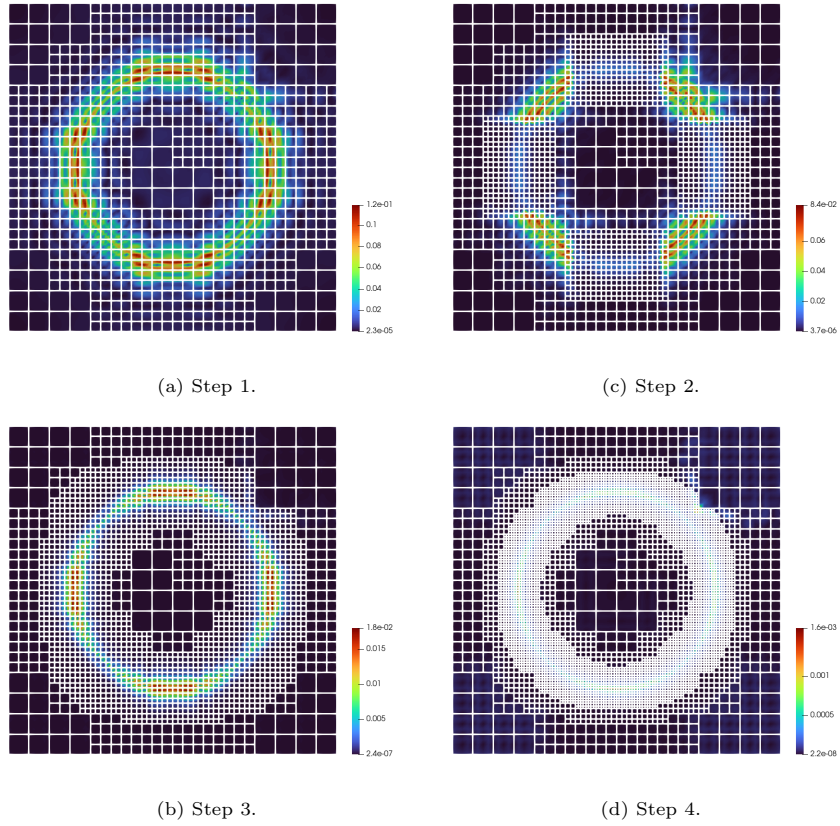


Figure 6: Adaptive refinement using Algorithm 1 for the vector Laplace problem with analytical solution (9). By adding L-chains according to Algorithm 1, we avoid the problematic intersections encountered in Fig. 5 and arrive at a similar final refined mesh in half the number of steps.

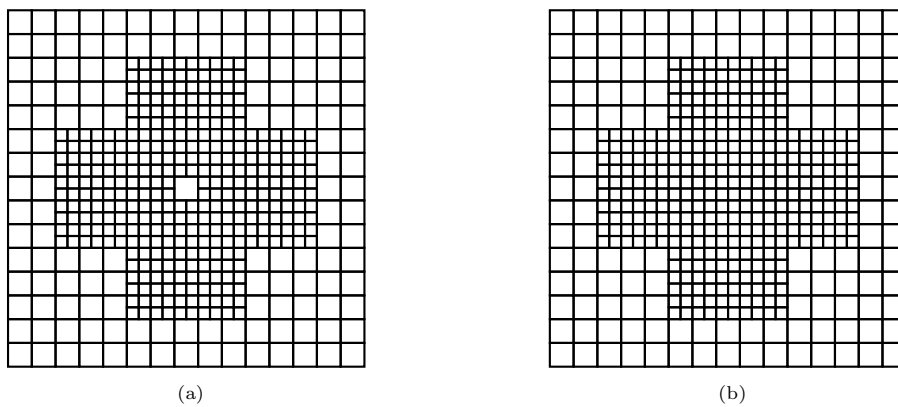


Figure 7: Two hierarchical meshes. The mesh in Fig. 7a has four problematic intersections while the one in Fig. 7b is the result of applying Algorithm 1 to the mesh in Fig. 7a and therefore has none.

the topology of the domain. We will also solve this problem on two distinct meshes, see Fig. 7, to highlight how spurious harmonic vector fields can alter the solution in subtler ways than before. After discretizing the relevant weak form, we wish to find $\omega_h \in \mathbb{R}$ and $\mathbf{u}_h \in \mathring{\mathbb{T}}_L^1$ such that

$$\langle \text{curl } \mathbf{u}_h, \text{curl } \mathbf{v} \rangle = \omega_h^2 \langle \mathbf{u}_h, \mathbf{v} \rangle, \quad \forall \mathbf{v} \in \mathring{\mathbb{T}}_L^1,$$

where $\mathring{\mathbb{T}}_L^1 := \mathbb{T}_L^1 \cap \mathring{\mathbf{H}}(\text{curl}; \Omega)$. We will use $p_{(\ell,k)} = 4$ for all ℓ and k . Due to the calculus identity $\text{curl } \mathbf{grad} \equiv \mathbf{0}$ and the boundary conditions on $\mathring{\mathbb{T}}_L^1$, the kernel of the operator is precisely composed of the gradients of functions in \mathbb{T}_L^0 with null-tangential components, because these are the gradients we can represent in $\mathring{\mathbb{T}}_L^1$. Which means that, after assembling our finite dimensional system, the number of null-eigenvalues in the spectrum is exactly $\dim(\mathbb{T}_L^0)$ minus the number of DoFs that contribute to values on the boundary. As such, after accounting for this offset, we can look at the eigenvalues given by solving the problem on the two meshes of Fig. 7. The results are shown in Table 1. It is important to mention that not only the null-space

Exact	Mesh Fig. 7a	Mesh Fig. 7b
1.000 000	0.000 000	1.000 000
1.000 000	0.000 000	1.000 000
2.000 000	0.000 000	2.000 000
4.000 000	0.000 000	4.000 000
4.000 000	1.000 000	4.000 000
5.000 000	1.000 000	5.000 000
5.000 000	2.000 000	5.000 000
8.000 000	4.000 000	8.000 000

Table 1: First 8 exact and computed eigenvalues for the maxwell eigenvalue problem using the meshes of Fig. 7. In this case, the non-null spectrum-rank offset is 429 and 456 for the two meshes, since $\dim(\mathbb{T}_L^0) = 501$ and $\dim(\mathring{\mathbb{T}}_L^1) = 528$, respectively, and the number of relevant boundary DoFs is 72 in both cases. Notice that the offset of mesh Fig. 7a is wrong by precisely 4 ranks, because the mesh has 4 problematic intersections. This is to be expected since each problematic intersection is responsible for introducing harmonic forms, which belong to $\ker(\text{curl})$.

offset is wrong, as shown in Table 1, but spurious eigenvalues are also introduced. The comparison between the two cases is shown in Fig. 8

8. Conclusions

A key ingredient in the construction of stable numerical methods for electromagnetics and fluid mechanics is the construction of a discrete de Rham complex that preserves the cohomology of the continuous one. While the construction of such complexes with tensor-product splines is well-understood, doing so with splines that allow for local refinement is not. In this paper, focusing on the use of (T)HB-splines in two dimensions, we have presented a first, constructive approach for building an adaptively-refinable discrete de Rham complex with the right cohomology.

Our approach builds upon recent results from [32]. They describe sufficient conditions for hierarchical meshes (in an arbitrary number of dimensions) such that the (T)HB-spline spaces built on them form an exact discrete de Rham complex. In two dimensions, given a hierarchical mesh which does not satisfy those conditions, we have now shown how it can be modified to do so. We have also presented algorithms that show how our theoretical results can be implemented. Moreover, we prove that, if the first space in the complex is of \mathcal{H} - or \mathcal{T} -admissibility class m , then so are the rest of the spaces. Ensuring admissibility is important not just from the point of view of the theory of hierarchical B-splines [12] but also for the stability of the numerical methods built on them [14]. Our theoretical results imply that the algorithms developed for maintaining admissibility of (T)HB-spline spaces (e.g., [6]) can be immediately used in the context of spline differential forms. Finally, we present numerical tests (both source and eigenvalue problems) that demonstrate the effectiveness of our approach.

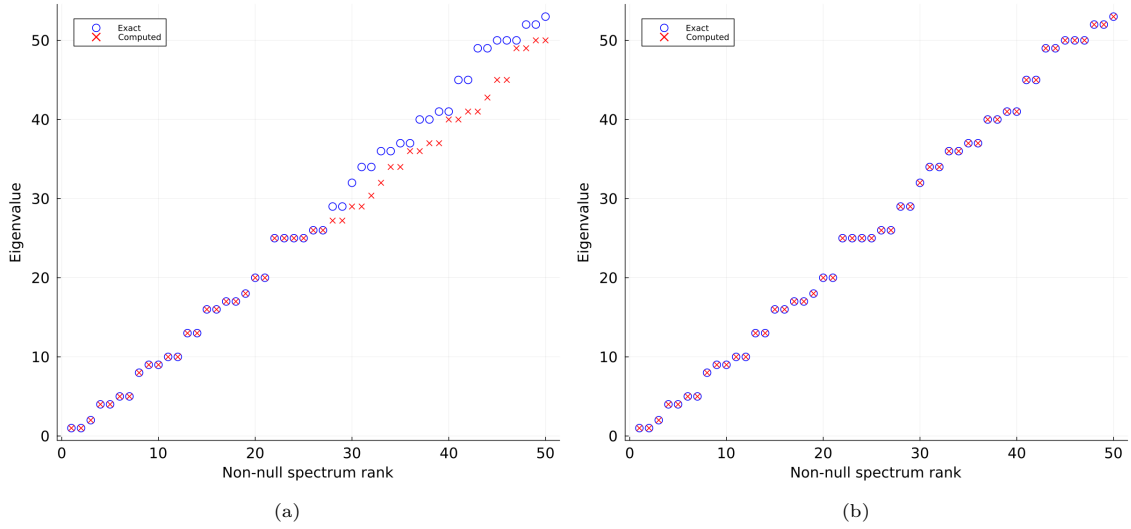


Figure 8: Comparison of the eigenvalues computed using the two meshes of Fig. 7. We are now accounting for both the offset of the gradients of scalar B-splines and the harmonic forms introduced by problematic intersections, which is 4 and 0 for the cases Fig. 7a and Fig. 7b, respectively. Once again, due to the 4 problematic intersections, we introduce 4 spurious eigenvalues, that in this case are around 27.2, 27.2, 30.4, and 42.8, completely meaningless values. This behaviour is of course not present when problematic intersections are absent.

There are several interesting lines of research that remain open. The construction of a discrete de Rham complex with THB-splines in three dimensions is a natural next step. It will also be interesting to study if the smallest quantum of refinement could be reduced from supports of 0-form B-splines to supports of volume-form B-splines, as was done in [20], thereby yielding slightly more flexible refinements. Another interesting research direction was alluded to at the end of Section 2: the formulation of bounded cochain projections for the hierarchical de Rham complex. These and other topics will be the subject of future work.

Acknowledgments

Diogo C. Cabanas is supported by grant number 2023.00238.BD awarded through the Portuguese Foundation for Science and Technology (FCT).

References

- [1] Douglas N. Arnold, *Finite element exterior calculus*, CBMS-NSF regional conference series in applied mathematics, no. 93, Society for Industrial and Applied Mathematics, SIAM, Philadelphia, 2018.
- [2] Douglas N. Arnold, Richard S. Falk, and Ragnar Winther, *Finite element exterior calculus, homological techniques, and applications*, Acta Numerica **15** (2006), 1–155.
- [3] ———, *Finite element exterior calculus: from Hodge theory to numerical stability*, Bull. Amer. Math. Soc. (N.S.), 47:281–354, 2010 **47** (2009), no. 2, 281–354.
- [4] Douglas N. Arnold and Ragnar Winther, *Mixed finite elements for elasticity*, Numerische Mathematik **92** (2002), no. 3, 401–419.
- [5] Carl De Boor, *A practical guide to splines*, rev. ed ed., Applied mathematical sciences, no. v. 27, Springer, New York, 2001, Includes bibliographical references (p. 331-339) and index.
- [6] Cesare Bracco, Annalisa Buffa, Carlotta Giannelli, and Rafael Vázquez, *Adaptive isogeometric methods with hierarchical splines: An overview*, Discrete & Continuous Dynamical Systems - A **39** (2019), no. 1, 241–261.
- [7] Susanne C. Brenner and L. Ridgway Scott, *The mathematical theory of finite element methods*, Springer New York, 2008.
- [8] Andrea Bressan and Espen Sande, *Approximation in FEM, DG and IGA: a theoretical comparison*, Numerische Mathematik **143** (2019), no. 4, 923–942.
- [9] A. Buffa, J. Rivas, G. Sangalli, and R. Vázquez, *Isogeometric discrete differential forms in three dimensions*, SIAM Journal on Numerical Analysis **49** (2011), no. 2, 818–844.
- [10] A. Buffa, G. Sangalli, and R. Vázquez, *Isogeometric analysis in electromagnetics: B-splines approximation*, Computer Methods in Applied Mechanics and Engineering **199** (2010), no. 17–20, 1143–1152.
- [11] Annalisa Buffa, Gregor Gantner, Carlotta Giannelli, Dirk Praetorius, and Rafael Vázquez, *Mathematical Foundations of Adaptive Isogeometric Analysis*, Archives of Computational Methods in Engineering **29** (2022), no. 7, 4479–4555.
- [12] Annalisa Buffa and Carlotta Giannelli, *Adaptive isogeometric methods with hierarchical splines: Error estimator and convergence*, Mathematical Models and Methods in Applied Sciences **26** (2015), no. 01, 1–25.
- [13] ———, *Adaptive isogeometric methods with hierarchical splines: Optimality and convergence rates*, Mathematical Models and Methods in Applied Sciences **27** (2017), no. 14, 2781–2802.
- [14] Massimo Carraturo, Carlotta Giannelli, Alessandro Reali, and Rafael Vázquez, *Suitably graded THB-spline refinement and coarsening: Towards an adaptive isogeometric analysis of additive manufacturing processes*, Computer Methods in Applied Mechanics and Engineering **348** (2019), 660–679.
- [15] Philippe G. Ciarlet, *The Finite Element Method for Elliptic Problems*, Classics in applied mathematics, no. 40, Society for Industrial and Applied Mathematics (SIAM, 3600 Market Street, Floor 6, Philadelphia, PA 19104), Philadelphia, Pa., 2002, System requirements: Adobe Acrobat Reader.
- [16] Willy Dörfler, *A Convergent Adaptive Algorithm for Poisson’s Equation*, SIAM Journal on Numerical Analysis **33** (1996), no. 3, 1106–1124.
- [17] Davide D’Angella, Stefan Kollmannsberger, Ernst Rank, and Alessandro Reali, *Multi-level Bézier extraction for hierarchical local refinement of Isogeometric analysis*, Computer Methods in Applied Mechanics and Engineering **328** (2018), 147–174.
- [18] Davide D’Angella and Alessandro Reali, *Efficient extraction of hierarchical B-splines for local refinement and coarsening of isogeometric analysis*, Computer Methods in Applied Mechanics and Engineering **367** (2020), 113131.
- [19] John A. Evans, Yuri Bazilevs, Ivo Babuška, and Thomas J.R. Hughes, *n-Widths, sup-inf, and optimality ratios for the k-version of the isogeometric finite element method*, Computer Methods in Applied Mechanics and Engineering **198** (2009), no. 21–26, 1726–1741.
- [20] John A Evans, Michael A Scott, Kendrick M Shepherd, Derek C Thomas, and Rafael Vázquez Hernández, *Hierarchical B-spline complexes of discrete differential forms*, IMA Journal of Numerical Analysis **40** (2018), no. 1, 422–473.
- [21] Gerald E. Farin, *Curves and surfaces for cagd*, 5. ed., [nachdr.] ed., The @Morgan Kaufmann series in computer graphics and geometric modeling, Morgan Kaufmann Publ., San Francisco, Calif. [u.a.], 2006, Includes bibliographical references (p. 449-489).
- [22] Carlotta Giannelli, Bert Jüttler, and Hendrik Speleers, *THB-splines: The truncated basis for hierarchical splines*, Computer Aided Geometric Design **29** (2012), no. 7, 485–498.
- [23] ———, *Strongly stable bases for adaptively refined multilevel spline spaces*, Advances in Computational Mathematics **40** (2013), no. 2, 459–490.
- [24] Thomas J. R. Hughes, *The finite element method*, Dover Publications, Mineola, NY, 2000, Reprint. Originally published: Englewood Cliffs, N.J. : Prentice-Hall, 1987.
- [25] T.J.R. Hughes, J.A. Cottrell, and Y. Bazilevs, *Isogeometric analysis: CAD, finite elements, NURBS, exact geometry and mesh refinement*, Computer Methods in Applied Mechanics and Engineering **194** (2005), no. 39–41, 4135–4195.
- [26] Les Piegl and Wayne Tiller, *The nurbs book*, Springer Berlin Heidelberg, 1997.
- [27] Espen Sande, Carla Manni, and Hendrik Speleers, *Sharp error estimates for spline approximation: Explicit constants, n-widths, and eigenfunction convergence*, Mathematical Models and Methods in Applied Sciences **29** (2019), no. 06, 1175–1205.
- [28] ———, *Explicit error estimates for spline approximation of arbitrary smoothness in isogeometric analysis*, Numerische Mathematik **144** (2020), no. 4, 889–929.
- [29] Larry Schumaker, *Spline functions: Basic theory*, Cambridge University Press, August 2007.
- [30] Thomas W. Sederberg, David L. Cardon, G. Thomas Finnigan, Nicholas S. North, Jianmin Zheng, and Tom Lyche, *T-spline simplification and local refinement*, ACM Transactions on Graphics **23** (2004), no. 3, 276–283.

- [31] Thomas W. Sederberg, Jianmin Zheng, Almaz Bakenov, and Ahmad Nasri, *T-splines and T-NURCCs*, ACM Transactions on Graphics **22** (2003), no. 3, 477–484.
- [32] Kendrick Shepherd and Deepesh Toshniwal, *Locally-verifiable sufficient conditions for exactness of the hierarchical B-spline discrete de Rham complex in \mathbb{R}^n* , Foundations of Computational Mathematics (2024).
- [33] Hendrik Speleers and Deepesh Toshniwal, *A general class of C^1 smooth rational splines: Application to construction of exact ellipses and ellipsoids*, Computer-Aided Design **132** (2021), 102982.